1 Functional Zones in the Extruder

1.1 Transport of Solids into and in the Extruder, Feed Limits

Reiner Rudolf, Carsten Conzen

During compounding, mainly solids, and in rare cases liquids or melts, are fed into the feed hopper located at the beginning of the twin-screw extruder. Furthermore, after the melting zone, additional solids can be fed into the extruder via side feeding units and liquids and gases can be injected via injection nozzles.

Twin screw extruders can be operated either starve fed or flood fed.

When run starve fed, less product is fed into the twin-screw extruder via the feed hopper than the screws can convey. Therefore, the feed zone is not completely filled with product.

Advantages include, for example, better recipe accuracy when dosing several components separately and higher flexibility due to the variable energy input caused by the variable throughput/speed ratio (filling degree) [1].

In flood fed operation, the extruder is operated with a fully filled feed hopper. This means that the screws convey as much product as their conveying capacity.

This section is limited to the description of the processes in the solids conveying zone at the beginning of the twin-screw extruder in starved feed operation, as co-rotating twin-screw extruders, unlike single-screw extruders, are generally operated in a starved feed condition.

As shown in Table 1.1, the solids to be dosed can be differentiated according to their particle shape and their melting behavior.

Table 1.1 Classification of Solids Fed into the Twin-Screw Extruder and Typical Examples

Particle shape	Melting behavior		
	Non-melting	**Low melting** *)	**Melting**
Pellet	Filler-masterbatches		Polymers
Powder	Filler, pigments	Waxes	Polymers
Flakes		Waxes	Polymers
Fiber	Glass, carbon		

*) melting point lower, ca. 100 °C

Usually, solids with different particle shapes and melting behavior are fed simultaneously into the twin screw extruder, e.g. melting polymer granulates together with non-melting filler powder and low-melting wax.

1.1.1 Characteristic Values and Calculation Possibilities

In order to determine the required speed range for a required throughput when operating in starved feed mode or to determine the maximum possible throughput at a given screw speed, it is necessary to know the solids conveying capacity. The intake capacity depends on the free cross-section between the screw elements and the barrel, A_{free}, the screw pitch T, the bulk density ρ_S, the conveying efficiency φ, and the screw speed n, and can be determined with Equation (1.1) [1].

$$\dot{M}_F = A_{free} \cdot T \cdot \rho_S \cdot \varphi \cdot n \tag{1.1}$$

However, this approach only applies to simple bulk solids without feed limitation with linear throughput/screw speed behavior (cf. Figure 1.3).

In co-rotating twin-screw extruders with axially open screw channels, the conveying efficiency in Equation (1.1) depends on the friction conditions of the solid with the inner cylinder surface and the screw surface as well as the inner friction of the solid. To achieve the highest possible conveying efficiency, the circumferential force between the cylinder surface and the solid must be as high as possible and the circumferential force between the solid and the screw as low as possible. This can be illustrated using a rotating threaded rod (screw) with a threaded bushing (solid) freely movable on it. The threaded bushing rotates without forward movement on the threaded rod, since the maximum friction force in the thread (screw–solid) is much larger than the maximum air friction on the outer threaded bushing (solid–cylinder). If the bushing is fixed, the possible force for fixing the bushing (solid–cylinder) is considerably greater than the frictional force in the thread (solid–screw), and the bushing is moved forward at the maximum possible axial speed. Thus, at pure axial flow the maximum conveying capacity in a screw system is determined by the bulk density, the free cross-sectional area, the screw pitch, and the screw speed.

$$\dot{M}_F = A_{free} \cdot T \cdot \rho_S \cdot n \tag{1.2}$$

The conveying efficiency can now be determined at a given throughput, screw speed, and bulk density of the polymer as follows:

$$\varphi = \frac{\dot{M}}{A_{free} \cdot T \cdot \rho_S \cdot n} \tag{1.3}$$

and is between 0 and 1 [1].

In co-rotating twin-screw extruders, the deflection of the solid through the 8-shaped contour of the cylinder exerts a resistance and thus an increased circumferential force between the solid and the cylinder. This reduces the tendency for the solid to slip off the cylinder wall and results in an increased axial movement of the solid. Tests have shown that with the usual powder, fine grained, and granular granulate fillings the conveying efficiency varies only slightly with the given screw geometry. This can be traced back to the big influence of the suppression of rotation. As can be seen in Figure 1.1, the conveying efficiency decreases with increasing screw pitch. According to Equation (1.1), the optimum pitch in the feed zone is defined by the product of the intake pitch and the conveying efficiency. Therefore, Figure 1.1 also shows the effective intake pitch as the product of the intake pitch and the conveying efficiency [1].

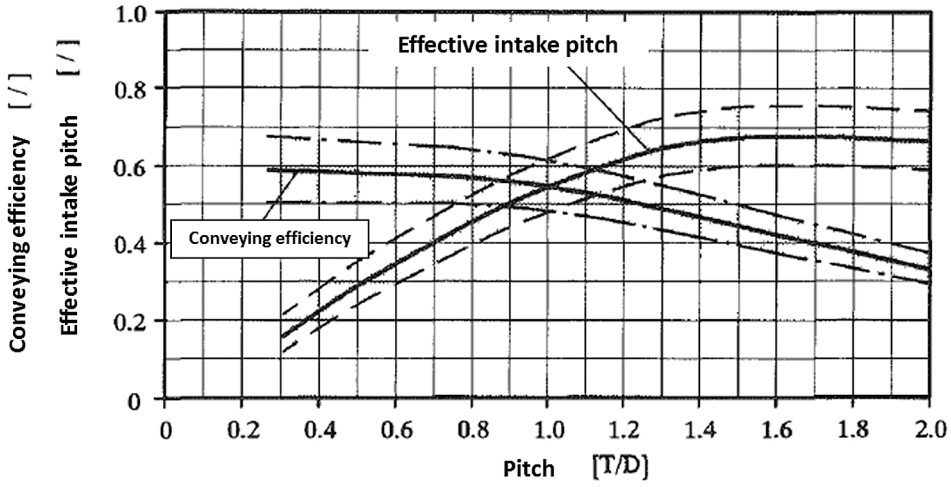

Figure 1.1 Conveying efficiency of co-rotating two- and three-lobed twin screw elements (effective intake pitch = conveying efficiency × intake pitch) [2]

At Covestro (formerly Bayer Technology Services), the solids conveying behavior was investigated experimentally in a co-rotating, tightly intermeshing twin-screw extruder with 58 mm screw diameter and plexiglass housings, with movies being taken from above, below, and from both sides. The selected screw had an initial pitch of 1.4 *D* with subsequent pitch reduction to 0.7 *D*. The investigated process conditions were simulated using DEM to determine the accuracy of the simulation. As can be seen from Figure 1.4 to Figure 1.7, experiment and simulation agree very well for all cases.

The different conveying angles of cylindrical and spherical granules are also reproduced very well, as Figure 1.8 shows.

Both experiment and simulation show that dosing fluctuations in the solids conveying zone cannot be compensated and, thus, have an effect at least up to the plasticizing zone (cf. Figure 1.9).

Due to the very good reproduction of reality, it is now possible to carry out screw design and process optimizations of the solids conveying zone of co-rotating twin-screw extruders for granular bulk materials by means of DEM simulation.

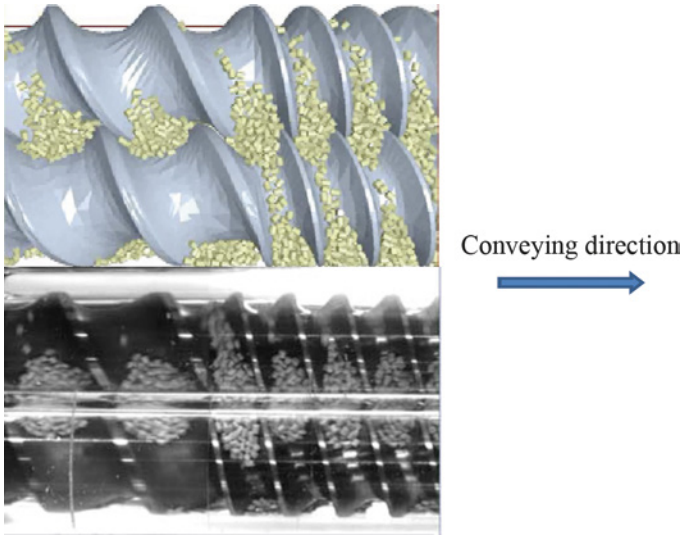

Figure 1.4 Comparison DEM simulation (top) with experiment (bottom) – top view

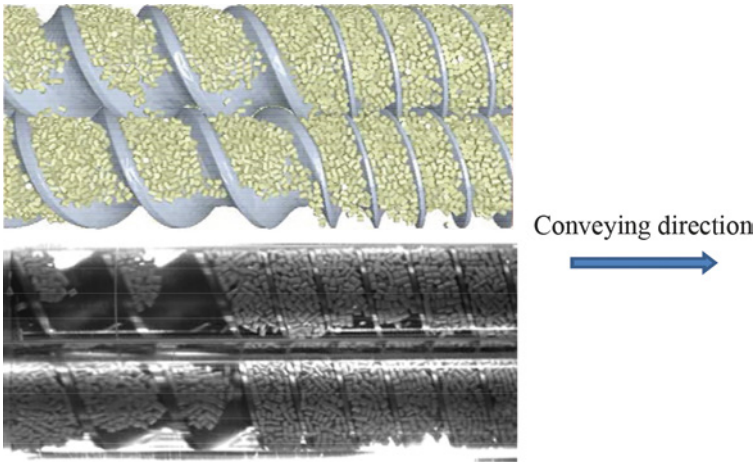

Figure 1.5 Comparison DEM simulation (top) with experiment (bottom) – view from below

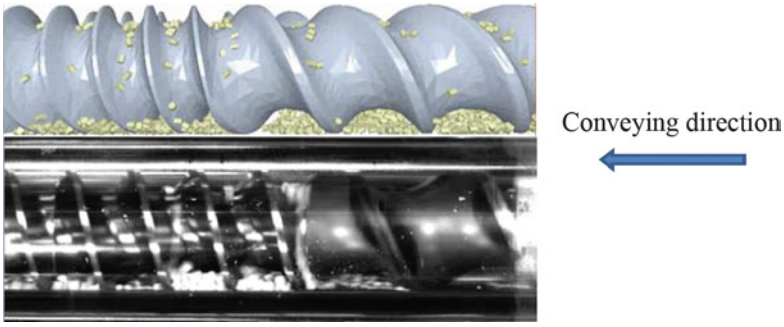

Figure 1.6 Comparison DEM simulation (top) with experiment (bottom) – left screw

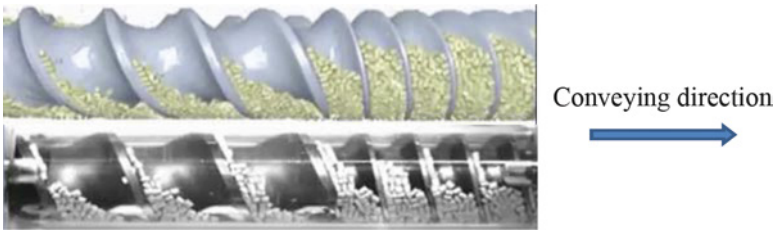

Figure 1.7 Comparison DEM simulation (top) with experiment (bottom) – right screw

In the position of the screws shown in Figure 1.35 the part of the sub-stream 3 represented by the cross-sectional area A_{32} no longer has a free surface. The free surface S_{31}^{PB} of the cross-sectional area A_{31} is larger than that of the fully developed liquid pool of the sub-streams 1 and 2. This is due to the greater radial distance of the surface of the screw profile from the inner barrel surface at this point compared to the fully developed liquid pool at this filling level. The free surfaces S_{21}^{SA} and S_{21}^{GO} have further decreased compared to Figure 1.33 and Figure 1.34. In contrast to Figure 1.34 on shaft 2 in screw channel 1 on the inside of the barrel surface and on the liquid layer of the screw element the new free surfaces S_{12}^{G0} and S_{12}^{SA} have been created. The point P_{32}^{PB} is no longer part of the sub-stream 3 and is now positioned on the free surface S_{12}^{SA}.

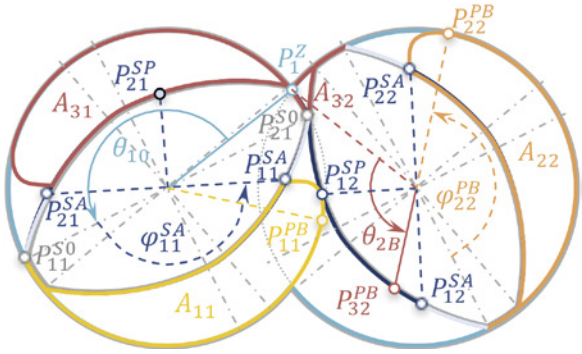

Figure 1.36 Liquid distribution in the cross-section of a twin-screw machine with double-flighted screw elements; degree of filling $\epsilon = 80\%$; rotational angle $\theta_{10} = \theta_P + \pi / i_g$

Figure 1.36 presents the liquid distribution in the position $\theta_{10} = \theta_P + \pi / i_g$. Compared to Figure 1.33, this corresponds to a rotation of $\Delta\theta = \pi / i_g$. The sub-stream 1 on shaft 1 hits the liquid layer in screw channel 1 on shaft 2 at point P_{12}^{SP}. This coincides phase-shifted with the liquid distribution shown in Figure 1.33. This process is repeated from one sub-stream to another depending on the number of threads i_g phase-shifted by π / i_g. The change from shaft to shaft takes place for each sub-stream by a rotation of the shafts of $\Delta\theta = \pi(2 - 1 / i_g)$. After a rotation of $\Delta\theta = 2\pi(2 - 1 / i_g)$ the sub-stream is again on the starting shaft but in the other screw channel. After a rotation of $\Delta\theta = 2\pi\left(2i_g - 1\right)$ the liquid pool is again on the same shaft in the same channel. With a double-flighted screw of $i_g = 2$ this identical situation to the start position is reached after three turns.

The free surfaces represent phase interfaces. They are necessary for the diffusive mass transport from the polymer melt into the gas phase. Concentration boundary layers are developed on these surfaces. For both the free surfaces of the liquid pools and for the liquid layers on the screw elements and the barrel that are temporarily covered by the liquid pool, it is assumed that the concentration boundary

layer is periodically mixed with the liquid pool. For complete mixing, the mean concentration of a liquid element reaching the phase interface is equal to the mean liquid concentration in the flow cross-section. Each of these periodically renewed elements thus fulfills the conditions of the model for the diffusive mass transport in polymers as described in Section 3.3 of *Co-Rotating Twin-Screw Extruders: Fundamentals*. Size and residence time of the liquid elements at the phase boundary must be known to determine the change in the mean concentration of the diffusing species in the devolatilization zone.

Both the surface of the liquid layer on the screw elements and the free surfaces of the liquid pools are helical surfaces. In a general form, these surfaces are defined with the independent parameters φ, ψ by the local vector $\vec{r}(\varphi,\psi)$ [1]:

$$\vec{r}(\varphi,\psi) = r(\varphi)\cos(\varphi+\psi)\vec{e}_x + r(\varphi)\sin(\varphi+\psi)\vec{e}_y + \left[h_g / (2\pi)\right]\psi\vec{e}_z \tag{1.24}$$

h_g indicates the thread height (pitch) of the screw. It corresponds to the axial length of a screw element for one winding ($\psi = 2\pi$) along the screw surface. For $r(\varphi)$ the functions for describing the shape of the liquid pool and the surface of the liquid layer on the screw elements have to be inserted. The used profiles are displayed in Figure 1.33 to Figure 1.36 The shape of the liquid layer on the screw surface results from the geometry of the screw elements, including the layer thickness. The shape of the free surface of the liquid pools is described with an empirical function that approximates the visually observed bead-like shape of the liquid pool.

With the partial derivatives

$$\vec{r}_\varphi = \partial\vec{r} / \partial\varphi \text{ and } \vec{r}_\psi = \partial\vec{r} / \partial\psi \tag{1.25}$$

of the local vector $\vec{r}(\varphi,\psi)$ follows for the surface element dS the relationship:

$$dS = \left|\vec{r}_\varphi \times \vec{r}_\psi\right| d\varphi d\psi \tag{1.26}$$

By numeric integration in the limits of φ and ψ one gets the surface S:

$$S = \iint \left|\vec{r}_\varphi \times \vec{r}_\psi\right| d\varphi d\psi \tag{1.27}$$

While the cross-sectional areas A for a screw profile are independent of the thread height h_g the surfaces S must be calculated as a function of h_g.

In order to obtain quantifiable information on the size of the phase interface, the relationship between filling degree and conveying behavior must be considered. Partial filling is always achieved with pressure less conveying if the condition for the volumetric flow number $\dot{V}^*$

$$\dot{V}^* < \dot{V}^*_{max} \tag{1.28}$$

2 Scale-up and Scale-down

2.1 Introduction and Basis Rules for Thermally Sensitive Products

Klemens Kohlgrüber

The scale-up of a process is an important step and will be found in several sections of this book. The focus is on the following question: how is a production machine to be designed so that the tests carried out with a smaller machine can be transferred to a production machine? The desired throughput with a necessary product quality is often in focus. The price of a large extruder usually correlates with the diameter of the machine. Therefore, the aim is usually that the production machine is as small as possible.

For the size of a machine, rough estimates with the following equation are often executed at the scale-up.

$$\frac{\dot{V}_Y}{\dot{V}_X} = \left(\frac{D_Y}{D_X}\right)^x \tag{2.1}$$

$\dot{V}_X$ is the throughput of the test machine with diameter D_X and machine "Y" is the production machine. The throughput ratio $\frac{\dot{V}_Y}{\dot{V}_X}$ is given based on the definition of the task. The diameter of the production machine D_Y at the given diameter of a test machine D_X depends strongly on the so-called scale-up exponent x: the smaller x is, the larger becomes D_Y. This is shown in a final example.

Empirical values are often given for the scale-up exponent x. For processes scaling predominantly with the product volume, it is close to 3; for surface-dominated processes (for example for the evaporation of volatile components) it will generally be lower. The ratio of area/volume is $1/D$ and gives an exponent 2. For heat transfer it can take the very unfavorable value 1.

In this book, Equation (2.1) is considered in several places, for example in Sections 2.2, 4.4, and 4.5.

Even without the consideration of specific processes, different exponents can be discussed if important basic principles are taken into account. In the following, some examples are given which include, amongst others, the dimensionless throughput, the geometric similarity, and the shear rate at the tip.

2.1.1 Dissimilarity

It is clear that not all functional zones of an extruder produce the same scale-up exponent. Therefore, a scale-up usually involves compromises. A scale-up can also be performed "dissimilarly" to the test machine so that the desired throughput with the necessary product quality is achieved. For example, the opening cross-section of an extruder housing behaves in relation to the volume in the extruder as 1/diameter. In the case of powder dosing, a feed limit can easily occur on a production scale. On a production scale, the feed opening can then be chosen to be geometrically dissimilar compared to the test machine; for example, the feed opening may be relatively larger (L/D larger) or the dosing may take place via two openings. If the material has a very low bulk density, the feed limit on a production scale can be so severe that the economic use of an extruder is not possible. In this case, special large-volume, high-viscosity reactors may be an alternative. This example makes it clear that in many cases it makes sense first to determine a suitable production machine and then to consider a scale-down for a suitable test machine.

2.1.2 Comparison of Production Machines

If the product development took place, for example, in a small type of device or machine, then quite different types of devices and machines could be considered for a large production machine. The "process requirement profile" must be compared with the "machine capability profile". Under the requirement profile, procedural aspects such as viscosity ranges, residence times, temperature control, mixing and dispersing, etc., need to be understood. In addition to the process aspect of feasibility on a production scale, many points play a role. Some points that should be considered when comparing production machines:

- Economic feasibility (includes many points; besides investment, also operating costs: personnel, energy, wear, availability, etc.)
- Process stability (degree of automation, complexity, constant product quality, etc.)

For the next step Potente and Preuß introduced formal relationships to compare the two machines and processes. Only the required relationships and ratios to explain the following method are presented here.

For the speed v:

$$v \sim Dn_0 \tag{2.49}$$

For channel width b:

$$b \sim D \tag{2.50}$$

$$\frac{b_1}{b_0} = \left(\frac{D_1}{D_0}\right) \tag{2.51}$$

For the channel depth h:

$$h \sim D^{\psi} \tag{2.52}$$

$$\frac{h_1}{h_0} = \left(\frac{D_1}{D_0}\right)^{\psi} \tag{2.53}$$

where ψ is the channel depth exponent.

For the screw speed

$$n_0 \sim D^{-\chi} \tag{2.54}$$

$$\frac{n_{0,1}}{n_{0,0}} = \left(\frac{D_1}{D_0}\right)^{-\chi} \tag{2.55}$$

where χ is the screw speed exponent.

Since the material properties and the pitch angle are assumed to be constant, the throughputs of the machines can also be set in relation to each other:

$$\frac{\dot{M}_1}{\dot{M}_0} = \frac{\dot{V}_1}{\dot{V}_0}\frac{\rho_1}{\rho_0}$$

$$\Rightarrow \frac{\dot{M}_1}{\dot{M}_0} = \left(\frac{D_1}{D_0}\right)^{\psi}\left(\frac{D_1}{D_0}\right)\left(\frac{D_1}{D_0}\right)\left(\frac{D_1}{D_0}\right)^{-\chi}$$

$$\Leftrightarrow \frac{\dot{M}_1}{\dot{M}_0} = \left(\frac{D_1}{D_0}\right)^{2+\psi-\chi} \tag{2.56}$$

where ρ represents the melt density.

The channel depth exponent ψ in Equation (2.56) is fixed due to the fixed geometries of model and target machine. The speed exponent χ must be determined based on the chosen boundary conditions. This will be discussed in Sections 2.2.3.2.2 and 2.2.3.2.5.

The consideration of the power inputs of both machines requires a consideration of the melt temperatures on both machines. Different solutions result for the individual conditions of the model and target machines in dependency on assuming the following:

- A constant or a variable melt temperature at the die outlet of both extruders
- A constant or variable pitch angle for both extruders

For example, based on the assumptions of a constant die outlet temperature of the melt and a constant pitch angle, the following solution results

$$\frac{P_1}{P_0} = \left(\frac{D_1}{D_0}\right)^{2+\psi-\chi} \tag{2.57}$$

For other assumptions regarding temperature and pitch angle, other solutions result, which are not discussed here. In this way, further model laws can be derived.

The model laws based on the assumptions of a constant melt temperature at the screw tip and a constant pitch angle are presented in Table 2.2.

Table 2.2 Model Laws for the Case of Constant Mass Temperatures at the Screw Tip and Constant Pitch Angle

Parameter		Model law
Throughput	$\frac{\dot{M}_1}{\dot{M}_0}$	$\left(\frac{D_1}{D_0}\right)^{2+\psi-\chi}$
Screw speed	$\frac{n_{0,1}}{n_{0,0}}$	$\left(\frac{D_1}{D_0}\right)^{-\chi}$
Power	$\frac{P_1}{P_0}$	$\left(\frac{D_1}{D_0}\right)^{2+\psi-\chi}$
Torque	$\frac{M_{D,1}}{M_{D,0}}$	$\left(\frac{D_1}{D_0}\right)^{2+\psi}$
Pressure	$\frac{p_1}{p_0}$	$\left(\frac{D_1}{D_0}\right)^{0}$
Temperature	$\frac{T_{1,1}-T_{0,1}}{T_{1,0}-T_{0,0}}$	$\left(\frac{D_1}{D_0}\right)^{0}$

3.1.4.1.2 Continuous Manufacture of Sealing Materials

Sealing compounds are commonly based on butyl rubber, polyisopropylene, polyurethane, or silicone rubber. Reactive sealing compounds can be crosslinked at room temperature (RTV) or at higher temperatures (HTV). Silicone sealing compounds are chemically hardening single-component systems in which the crosslinking of the substrate is initiated using moisture from the air. As a result, the reaction products are separated. After rapid skin formation on the surface, the crosslinking within the compound continues until hardening is complete. Areas of use include joint sealants in plumbing, construction, and the automobile industry.

Silicone sealing compounds such as those used, for example, in housing construction for sealing plumbing fixtures, are increasingly being manufactured in twin-screw extruders. Silicone polymer (30–50%), silicone oil (35–40%), crosslinking agents, and catalyst components are dosed into the extruder in fluid form using injection nozzles. In the process, the catalyst that reactively activates the mixture is worked in only at the end. As a rule, fillers such as silica (5–10%) create intake problems due to their very low fill density of approximately 50 g/l; they fluidize very easily and carry a great deal of air into the extruder which must then be removed again. A ZSK Mv's deeply cut flights enable significantly better powder intake and thus a throughput increase of over 35% as well compared to a ZSK Mc with an equal center distance. Discharge occurs during cartridge filling by means of a gear pump with a downstream heat exchanger and buffers directly into the cartridge filling unit. Additionally, masses can still be strained.

Typical throughputs for a ZSK 98 Mv sit at 2.6 t/h. Figure 3.15 shows one example of high dosing effort typical for this application.

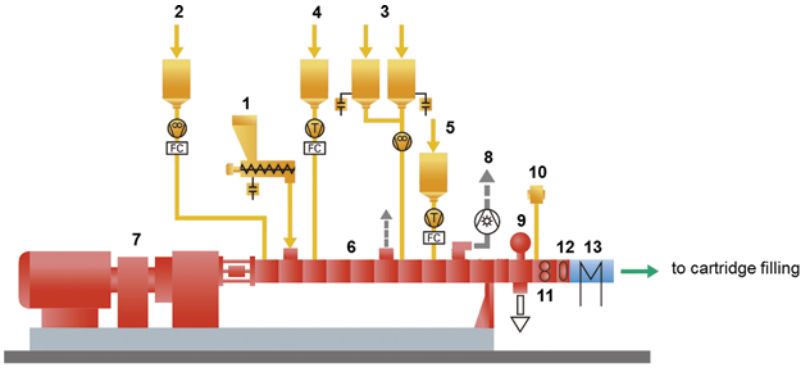

1 Grav. dosing Aerosil
2 Grav. dosing Silicone pol.
3 Grav. dosing Silicone oil
4 Grav. dosing crosslinker
5 Grav. dosing catalyst
6 Extruder ZSK MEGAvolume
7 Maindrive and Gearbox
8 Vacuum unit
9 Start-up-valve
10 On-line viscosimeter
11 Gearpump
12 Screen-pack-changer
13 Heat-exchanger

Figure 3.15 Example of silicone sealing compounds manufacture

3.1.4.2 Chemical Reactions in Twin-Screw Extruders

The reactive extrusion in ZSK-type twin-screw extruders is used for polymerization in the compound originating from monomers or pre-polymerizates, as well as for modification of polymers using grafting, crosslinking, and degradation. The demands upon a continuous reaction system vary according to the processing task.

3.1.4.2.1 Manufacture of Thermoplastic Polyurethane (TPU)

The ZSK allows for continuous manufacture of an extremely wide product spectrum, from soft polyurethane adhesives to the hardest thermoplastic polyurethane elastomers with Shore hardnesses of D60. These linear, thermoplastic polyurethanes are used as construction materials of varying hardness, as highly elastic coating materials, and for fibers and films. The manufacturing process (see also Figure 3.16) requires stoichiometric dosing of components, polyol (usually premixed with a catalyst), and diisocyanates in the fluid or melted state into the ZSK's feed.

The TPU manufacturing process can be expanded to incorporate further additional materials such as stabilizers, lubricants, dyes, and flame retardants that can be added downstream from the main intake via the side feeder (ZS-B) into the melt flow as required.

Discharge takes place via a gear pump and a screen pack changer directly into underwater pelletizing.

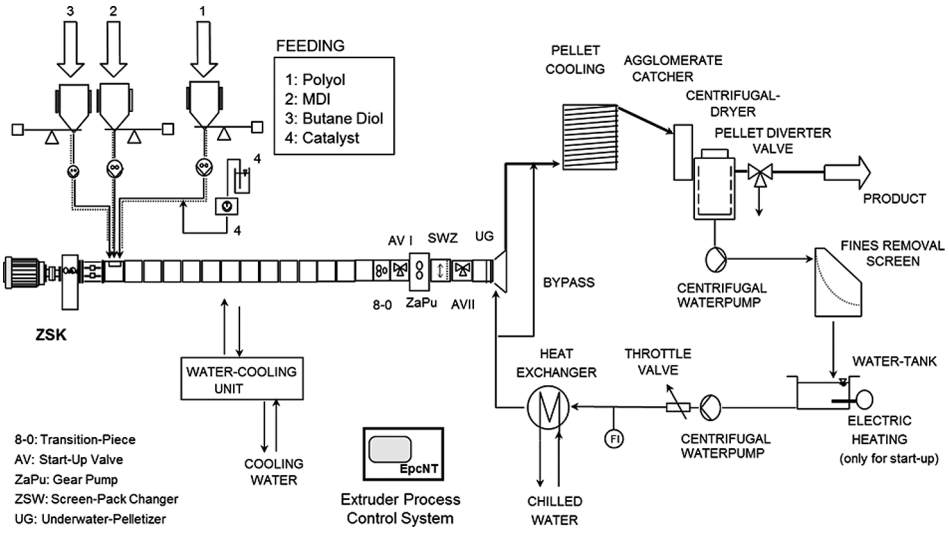

Figure 3.16 Plant for continuous manufacture of linear thermoplastic polyurethane

layer structures. Therefore, it is important to minimize the mechanical stress and shear during the incorporation processes in such a way that particle assemblies are broken up and distributed, but the micro structure of the particles remains intact. Consequently, mixtures of organic pigments and effect pigments represent a special case for dispersion, because the optimum processing conditions of the two product groups can be diametrically opposed.

4.2.2.1.1 Color Index and Particle Sizes: Pigments at First Glance

Organic pigments are assigned to a color index (C.I.) based on their chemical structure. The color index bears the color theme and a consecutive number. Pigments with the same C.I. can yet have different crystal morphologies and particle size distributions (→ electron micrographs of C.I. Pigment Red 202 and C.I. Pigment Purple 19: Figure 4.11, Figure 4.12). Therefore, the C.I. alone does not give conclusive information about the dispersion behavior of a pigment. Other pigment properties such as opacity, transparency, or hue can also be considerably different with the same C.I.

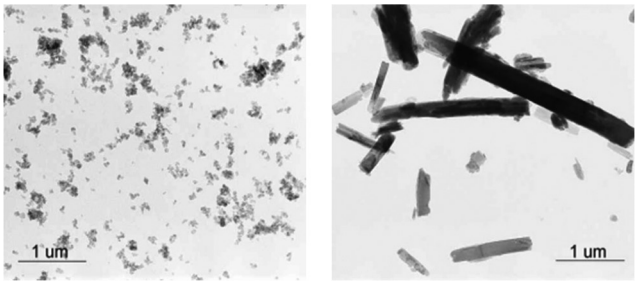

Figure 4.11 Different types of C.I. Pigment Red 202 [BASF AG]

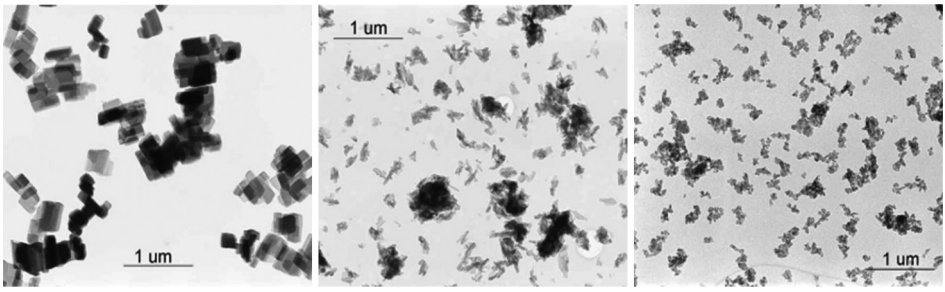

Figure 4.12 Different types of C.I. Pigment Purple 19 [BASF AG]

Commercially available powder pigments consist of a mixture of primary crystals, aggregates, and agglomerates. Primary crystals are individual crystals that are clearly described by their crystal structure and morphology. Primary crystals that have grown together at the corners and across common surface areas are called aggregates. They are firmly coalesced and can hardly be separated mechanically. Agglomerates are combinations of primary crystals and aggregates. They constitute the major part of powder pigments and, in the dispersion process, need to be broken down into primary crystals and aggregates as completely as possible.

4.2.2.1.2 Qualitative Description of the Dispersion Quality in a Masterbatch

When is an organic pigment well dispersed? This is generally the case when the color properties and fastnesses specified by the manufacturer have been achieved. The properties are tested in specified pigment concentrations in accordance with industrial guidelines and standards. For this purpose, the masterbatch has to be incorporated into defined polymers for testing. Especially hue, purity, tinting strength, as well as opacity or transparency, if required also heat resistance, light and migration fastness, should be checked by the colorist or the application engineer and fall within the scope of the manufacturer's specifications. Furthermore, no implications of poor dispersion should be visible at all when the masterbatch is compounded for testing at final concentration, such as:

- Streaks, specks, dots
- Low brilliance
- Hue shift
- Changed transparency/opacity
- Impairment of mechanical properties, failure in thin layers such as film tears or fiber breakage

Figure 4.13 below shows a typical particle size distribution of an organic pigment after dispersion. Maximum tinting strength and purity are achieved with a preferably large amount of particles around 0.1 µm. Particles in the range of 0.2 to 0.5 µm contribute to the opacity of the pigment. Fine particles that would impair the migration fastness are rarely generated by the dispersion process. Microscopically visible particles > 10 µm mainly cause the above-mentioned implications of poor dispersion. However, there is no direct correlation between the frequency of microscopically visible particles and the color strength of the masterbatch. This important fact will be taken up again in the considerations below.

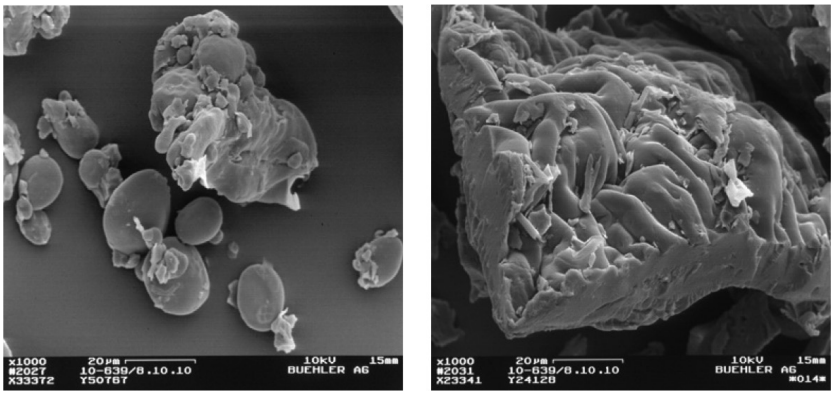

Figure 4.56 Left: natural wheat starch with visible starch granules and protein particles; right: extruded, cooked wheat starch [Bühler AG]

The many reasons behind the success of extrusion cooking are described in more detail in [4]. Here, we give a brief summary of the main ones:

1. Combination of the different basic process technology operations
2. Process and product flexibility
3. Low production and investment costs
4. Energy efficiency and sustainability

Cold extrusion for the production of pasta products, for instance, is based on the same physical principles and basic process technology operations as extrusion cooking. Semolina (200 to 500 µm) is mixed with water (30 to 33%), kneaded, and formed at a die pressure of approximately 110 bar. This process exposes the dough to mechanical and thermal energy, which, unlike extrusion cooking, causes little protein and starch damage. For this reason, the dough temperatures remain below 50 °C. The aim of cold extrusion is to produce dough with a continuous protein matrix which entraps the starch granules. In extrusion cooking, the process is the exact opposite and it is the starch that serves as a binder, rather than the protein.

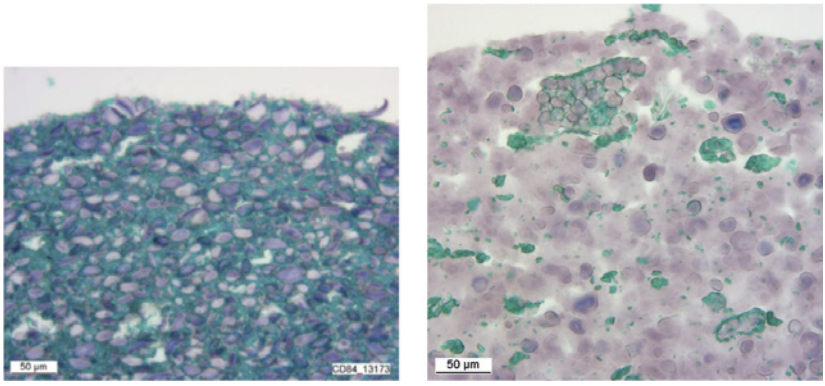

Figure 4.57
Left: cold extrusion – continuous protein matrix (green) with embedded starch granules (purple)
Right: hot extrusion – continuous starch matrix (purple) with embedded protein bodies (green)
[Bühler AG]

4.6.1 Extrusion of Breakfast Cereals

Preferences regarding breakfast tend to differ depending on the culture. However, breakfast cereals play a significant part. Studies show that annual consumption in Germany amounts to 1 kg per person per year. Cereals are eaten daily in 15% of households, once a week in 33% of households, and at least once a month in 10% of households. Interestingly, 50% of breakfast products made for children are consumed by adults [5].

Based on the example of a modern plant for extruded breakfast cereals, the following sections describe the process steps required to produce end products from the raw materials.

This type of extruder comprises the following process steps:

1. Preparation of raw materials and mixing
2. Preconditioning and extrusion
3. Tempering and flaking
4. Drying and spraying
5. End drying and roasting

The process flow chart in Figure 4.58 illustrates this type of system.